Icarus **148**, 589–593 (2000)
doi:10.1006/icar.2000.6535, available online at http://www.idealibrary.com on IDEAL®

NOTE
Slowly Rotating Asteroid 1999 GU_3

Petr Pravec and Lenka Šarounová

Astronomical Institute, Academy of Sciences of the Czech Republic, CZ-25165 Ondřejov, Czech Republic
E-mail: ppravec@asu.cas.cz

Lance A. M. Benner, Steven J. Ostro, Michael D. Hicks, Raymond F. Jurgens, Jon D. Giorgini, Martin A. Slade, and Donald K. Yeomans

Jet Propulsion Laboratory, California Institute of Technology, Pasadena, California 91109

David L. Rabinowitz

Yale University Physics Department, P.O. Box 208121, New Haven, Connecticut 06520-8121

Yurij N. Krugly

Astronomical Observatory, Kharkiv National University, Sumska Street 35, Kharkiv 61022, Ukraine

and

Marek Wolf

Astronomical Institute, Charles University Prague, V Holešovičkách 2, CZ-18000 Praha, Czech Republic

Received April 13, 2000; revised September 11, 2000

Optical and radar observations reveal that 1999 GU_3 is sub-kilometer-sized object with a synodic period of 9.0 days, low visual and radar albedos, and colors more consistent with the ordinary chondrites than the vast majority of main-belt asteroids.

Key Words: **asteroids, rotation; photometry; radar.**

1. Introduction. Studies of the distribution of asteroid spin rates vs diameter have shown that there is a significant excess of slow rotators with periods >30 h at diameters below ≈50 km (Dermott *et al.* 1984, Binzel *et al.* 1989, Fulchignoni *et al.* 1995, Pravec and Harris 2000). Asteroid collisional evolution models explain small asteroids as fragments generated in catastrophic disruptions or cratering of larger asteroids and predict their spin-up but not significant numbers of slow rotators (Harris 1979, Farinella *et al.* 1992). Mechanisms causing spin-down of small asteroids have been suggested (see Discussion below) but none of the hypotheses has been proven to satisfactorily explain the basic observational data.

The largest known slow rotator is C-type main belt Asteroid 253 Mathilde, which has a rotation period of 17.41 days and a mean diameter of 53 km (Mottola *et al.* 1995, Veverka *et al.* 1997). The best-studied slow rotator is S-type near-Earth Asteroid 4179 Toutatis, which radar observations have shown to be an elongated body in a nonprincipal axis (NPA) rotation state characterized by periods of 5.37 days (rotating about the long axis) and 7.42 days (precession of the long axis about the angular momentum vector; Hudson and Ostro 1995, Ostro *et al.* 1999a). Toutatis' NPA rotation causes its lightcurve to appear nonperiodic but it contains characteristic frequencies (corresponding to the observed synodic periods of 7.3 and 3.1 days) that are related to the periods of the NPA rotation (Spencer *et al.* 1995, Kryszczyńska *et al.* 1999).

Lightcurves of several other asteroids with long periods have shown deviations from simple periodicity that are suggestive of NPA rotation: 1689 Floris-Jan (Harris 1994), 288 Glauke and 3288 Seleucus (Harris *et al.* 1999), and 3691 Bede and 1997 BR (Pravec *et al.* 1998). Thus, although we cannot say that all slowly rotating asteroids are in NPA rotation states, such states appear to be common among them.

The size distribution of very slow rotators extends from Mathilde (≈50 km) down to 1997 BR (≈1.5 km, Pravec *et al.* 1998). Here we present observations of the ≈0.5 km object 1999 GU_3 that reveal a very slow rotation of 9 days.

2. Optical observations. We observed 1999 GU_3 photometrically from 1999 April 14.3 to May 19.9. The observations were made at Ondřejov Observatory, Kharkiv Observatory, and Table Mountain Observatory. We used telescopes with diameters of 0.6–0.7 m that are equipped with CCDs. The observations were made and reduced in the standard way as described by Pravec *et al.* (1996) and Rabinowitz (1998). The measurements were calibrated in the Johnson–Cousins system and calibrated using Landolt (1992) standards. Most observations were made through the R filter, with additional measurements in B, V, and I on April 14 and 15 at Table Mountain Observatory. The consistency of the R data calibrations from all three stations is about 0.02 mag. The times have been corrected for light travel time, and magnitudes have been reduced to unit geocentric and heliocentric distances. Table I summarizes the optical observations.

Figure 1A plots lightcurve measurements reduced to a phase angle of 60° (assuming a linear phase parameter of 0.031 mag/deg; see below) vs time. The relatively densely covered part of the lightcurve obtained between April 14 and 24 shows a long-period, large amplitude variation. If we assume that there are two maxima/minima pairs per cycle, then this 10-day interval appears

0019-1035/00 $35.00

TABLE I
Geometric Circumstances of Optical Observations

Date UT	RA h m	DEC ° ’	L_{PAB} (°)	B_{PAB} (°)	Δ (AU)	r (AU)	α (°)	Error (mag)	Observatory
1999 Apr. 14.4	15 57.8	36 58	211.6	29.1	0.0427	1.0263	55.9	0.01	Table Mountain
14.9	16 09.8	37 27	213.1	30.0	0.0448	1.0263	57.7	0.01	Ondřejov
15.4	16 20.9	37 50	214.6	30.7	0.0470	1.0264	59.3	0.01	Table Mountain
16.9	16 48.8	38 28	218.5	32.4	0.0538	1.0268	63.1	0.02	Kharkiv
17.9	17 03.8	38 37	220.9	33.2	0.0585	1.0273	65.0	0.02	Ondřejov
18.0	17 05.2	38 37	221.1	33.3	0.0590	1.0273	65.1	0.01	Kharkiv
18.9	17 16.5	38 38	223.1	33.8	0.0634	1.0279	66.4	0.01	Kharkiv
19.0	17 17.6	38 38	223.3	33.9	0.0639	1.0279	66.5	0.01	Ondřejov
20.0	17 28.2	38 34	225.3	34.4	0.0688	1.0287	67.6	0.01	Ondřejov, Kharkiv
21.0	17 37.4	38 27	227.2	34.8	0.0739	1.0296	68.4	0.01	Kharkiv
21.1	17 38.2	38 27	227.4	34.8	0.0744	1.0297	68.5	0.01	Ondřejov
23.1	17 52.6	38 09	230.8	35.3	0.0846	1.0320	69.4	0.02	Ondřejov
24.1	17 58.4	37 59	232.3	35.5	0.0897	1.0333	69.6	0.01	Ondřejov
May 4.1	18 30.5	36 20	244.7	35.9	0.1412	1.0541	67.4	0.04	Ondřejov
6.1	18 33.6	36 02	246.7	35.8	0.1513	1.0598	66.4	0.04	Ondřejov
8.1	18 36.1	35 44	248.6	35.7	0.1613	1.0659	65.3	0.05	Ondřejov
10.1	18 38.0	35 26	250.5	35.6	0.1712	1.0726	64.1	0.08	Ondřejov
17.1	18 41.6	34 21	256.2	35.1	0.2052	1.0993	59.6	0.04	Ondřejov
19.0	18 41.9	34 02	257.5	34.9	0.2143	1.1075	58.3	0.03	Ondřejov

Note. Δ and r are the geocentric and heliocentric distances and α is the solar phase angle.

to cover slightly more than one cycle. Realizing that we needed additional data to determine the rotation period more precisely, we observed the asteroid on six more nights from 1999 May 4 to 19. Due to telescope schedules and the short duration of the observing intervals on each night, we obtained only one point (that is the average of several measurements taken in quick succession) on each of the May nights. The May data show a large variation of the asteroid's brightness that is even larger than the amplitude seen in April.

We obtained the following mean color indices at Table Mountain on 1999 April 14.4 and 15.4: $B - V = 0.819 \pm 0.013$, $V - R = 0.438 \pm 0.01$, and $R - I = 0.250 \pm 0.02$. The distinct spectral absorption longward of 0.7 μm is presumably characteristic of the olivine/pyroxene composition of ordinary chondrites and of the QRV asteroid types.

Since the solar phase angle varied over a relatively narrow range between 56° and 70° during the optical observing window (Table I), we assumed that the asteroid's phase relation is linear with a coefficient of 0.031 mag/deg, corresponding to a phase slope parameter $G = 0.15$. We experimented with phase parameters varied by ± 0.003 mag/deg about this value (corresponding to G between -0.05 and 0.35, the range that is observed for most asteroids; Bowell *et al.* 1989) and found that our assumption did not introduce any significant systematic error to the results. The uncertainty of 0.003 mag/deg in the linear phase coefficient propagates as a relative error of 0.04 mag between reduced points of 1999 April 14.4 and 24.1, the epochs corresponding to the minimum and maximum solar phase angles observed. Accounting also for possible calibration errors (see above), we consider 0.05 mag as a likely maximum error of points in the reduced lightcurve during the analysis reported below; the only exception is the May 10.1 point that has a random error of 0.08 mag (see Table I). The mean error of all points in the reduced lightcurve is about 0.03 mag.

We searched for a period in the data using a Fourier series method (Harris *et al.* 1989). Figure 1B plots χ^2 (for a fit with a fourth-order Fourier series) vs period. There are two possible periods: 4.49 ± 0.01 and 9.03 ± 0.03 days. The shorter period corresponds to a lightcurve with a single maximum/minimum pair per cycle. Large-amplitude lightcurves dominated by the first harmonic are virtually unknown among asteroids and there is no plausible hypothesis how they could be generated (a large hemispheric albedo difference is not plausible for the small object), so we consider it likely that the shorter period solution corresponds to one-half of the synodic period of (9.0 ± 0.1) days, where we have adopted an error a few times larger than the formal statistical error to account for possible systematic effects (e.g., change of the synodic period with time) that are not incorporated in the model. The difference between the synodic and sidereal periods could be significant for this long-period, fast-moving object; from the motion of the phase angle bisector (PAB; Table I), we estimate that the synodic–sidereal difference could be as large as ± 0.25 day.

Figure 1C plots the composite lightcurve for a period of 9.0 days. The peak-to-trough amplitude is about 1.4 mag and it is consistent with an elongated shape. Most of the lightcurve points are from a single cycle between April 14 and 21. Points from the other cycles agree well with the same lightcurve except for the points on 1999 May 4.1 and 8.1 (plus symbols at phases 0.23 and 0.67, respectively, in Fig. 1C). The May 8.1 point is fainter by 0.36 mag than the average of points taken on April 20.0 and May 17.1 that occur around the same phase (0.67) in the composite lightcurve. This difference is much greater than its uncertainty—even if the phase effect was different from the $H - G$ relation (see above), that cannot explain the deviation because the April 20.0 and May 17.1 points were obtained at solar phase angles different by $+2.3°$ and $-5.7°$, respectively, from the phase angle of the May 8.1 point (see Table I). Thus, a different magnitude of the phase effect that would lessen the deviation of the May 8.1 point from one of the April 20.0 and May 17.1 points would enlarge the deviation from the other point. Thus, the deviation is likely real and it indicates that the asteroid's brightness was significantly lower on May 8.1 than at the same phase two cycles earlier and one cycle later. The point on May 4.1 (at phase 0.23 in Fig. 1C) is fainter than expected relative to adjacent points if we assume a smooth shape of the lightcurve at phases between 0.1 and 0.35. Although incomplete coverage of the cycle that includes the points on May 4.1 and 8.1 does not allow us to draw firm conclusions, it seems possible that both maxima (near phases 0.2 and 0.7 in Fig. 1C) had significantly lower levels during that cycle than during the cycles 18 days before and (in the case of the maximum at the phase 0.7) 9 days later. Change of lightcurve shape due to a change of aspect (the PAB changed by 19° from April 20.0 to May 8.1) does not explain the deviation well because the point of May 17.1 agrees with the points of April 20.0. The discrepancy of the May 4.1 and 8.1 points with the rest of the lightcurve hints that the asteroid's rotation may be complex. This conjecture needs to be confirmed by further observations.

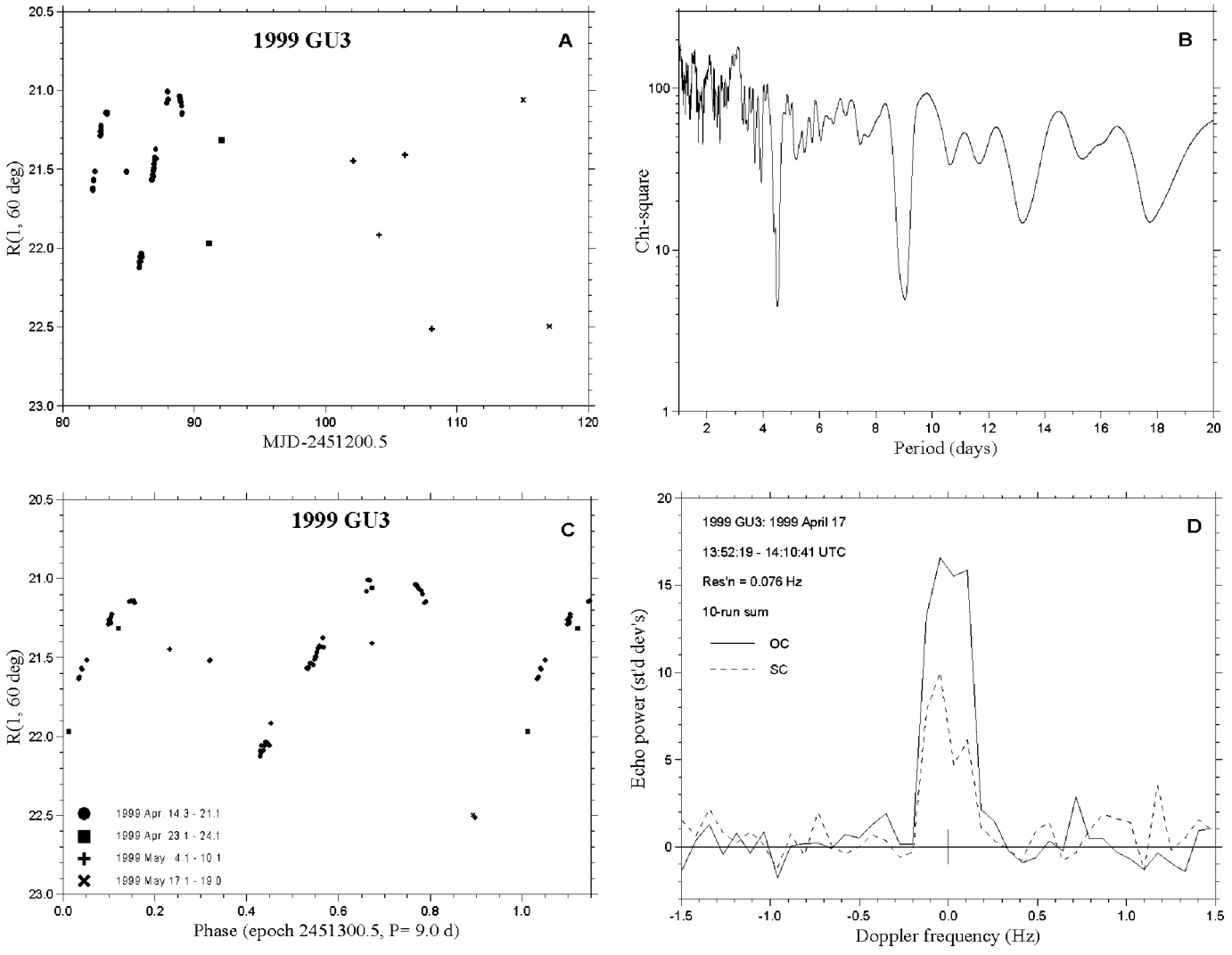

FIG. 1. Lightcurve of 1999 GU_3 (A) vs time and (C) phased with a period of 9.0 days. Each point is an average of several measurements taken in quick succession. (B) Sum of square residuals of the lightcurve points to the best-fit fourth-order Fourier series vs period. (D) Goldstone echo power spectrum of 1999 GU_3 at 0.076 Hz resolution. Echo power is plotted in standard deviations versus Doppler frequency relative to the estimated frequency of echoes from the asteroid's center of mass, which was estimated by eye using the middle of the Doppler cells exceeding five standard deviations. Solid and dashed lines denote echo power in the OC and SC polarizations.

We derived a mean absolute magnitude $H = 19.8 \pm 0.5$ from the zeroth order of the best fit Fourier series extrapolated to zero solar phase angle and by assuming $G = 0.15 \pm 0.2$.

3. Radar observations. We observed 1999 GU_3 with Goldstone's 8560-MHz (3.5-cm) radar system on 1999 April 17 at a distance of 0.057 AU (Table II). Our methods of radar data reduction and analysis followed those described in detail by Ostro *et al.* (1992). In Doppler-only or continuous wave (cw) observations, echoes were received simultaneously in the opposite (OC) and same (SC) senses of circular polarization as the transmission. We began with a wide bandwidth to ensure that the echo would fall within the receiver's passband and we obtained echoes with a correction of $+1172 \pm 30$ Hz to our initial Doppler prediction ephemeris, which was based on JPL orbit solution 10; this correction was comparable to the estimated $1 - \sigma$ uncertainty. We promptly used that measurement to generate a new ephemeris (solution 12). Subsequent analysis revealed that the echo was drifting in Doppler frequency relative to solution 10 by $\approx$1.5 Hz/h, which could have corrupted estimation of the echo bandwidth and interpretation of the echoes had the drift gone unnoticed. Therefore, except for the initial astrometry, where we assigned an appropriately large uncertainty, we did not use the cw echoes obtained with solution 10 in our analyses. We completed 10 more cw runs using solution 12, measured a Doppler correction of 12.1 ± 0.2 Hz at the epoch 1999 April 17 14:00:00 UTC, and concluded the experiment by attempting (unsuccessfully) to measure the asteroid's range. The Doppler astrometry is available at the JPL Solar System Dynamics website at http://ssd.jpl.nasa.gov/radar_data.html (Chamberlin *et al.* 1997).

Figure 1D shows an echo power spectrum of 1999 GU_3. A weighted sum of 10 cw runs gives an OC radar cross section $\sigma_{OC} = 0.014 \pm 0.007$ km^2; uncertainties are dominated by systematic pointing and calibration errors, and we assign standard errors of 50% to the estimates. The asteroid's circular polarization ratio $SC/OC = 0.36 \pm 0.07$ (the uncertainty is due to receiver noise) is larger than $\approx$70% of the NEA ratios reported in the peer-reviewed literature (Benner *et al.* 1999b), and it indicates that the near-surface of 1999 GU_3 at decimeter scales is morphologically rougher than those of most radar-detected NEAs.

The spectrum resolves the asteroid into four 0.076-Hz Doppler cells exceeding five standard deviations and establishes a bandwidth of 0.3 Hz. Narrow bandwidth requires either that 1999 GU_3 is a very slow rotator, that the apparent

TABLE II
Radar Observations

Date UT	RA h m	DEC ° ’	Δ (AU)	P_{tx} (kW)	Band (Hz)	OSOD soln	Runs	Δt (UTC h)	Δf (Hz)	TXoff (Hz)
1999 Apr. 17.6	16 59.6	38 35	0.0571	438	20000	10	8	09.06–09.30	9.8	0
					20000	10	28	09.34–10.21	9.8	−1171.875
					5000	12	10	13.87–14.18	4.9	0

Note. Times are the mid-epochs of the observations, given to the nearest one-tenth of a day. The geocentric right ascension and declination are given for equinox J2000. Δ is the geocentric distance. P_{tx} is the average transmitter power and Band is the sampling rate. The orbital solution number is given in column seven. The number of transmit–receive cycles (runs) is listed in the eighth column. Δt is the interval spanned by each type of observation, Δf is the raw frequency resolution in the real-time display, and TXoff is the transmitter frequency offset.

spin vector was near the line of sight, and/or that the effective diameter is smaller than the *a priori* estimate of several hundred meters.

1999 GU_3 was not resolved in range, but the echo bandwidth (given by $B = 4\pi D \cos\delta/(\lambda P)$, where D is the breadth of the object, δ is the subradar latitude, λ is the radar wavelength, and P is the rotation period) and rotation period of 9 days place a lower bound on the maximum pole-on breadth $D_{\max} \geq 0.64$ km. If we assume that the effective diameter (the diameter of a sphere with the same projected area as the target) $D_{\rm eff} = D_{\max}$ and we adopt the 1-σ upper limit on $\sigma_{\rm OC}$ and the formal lower limit on H, then we obtain upper bounds on the radar albedo (equals to $\sigma_{\rm OC}$/projected area) and visual geometric albedo (computed from $\log p_v = 6.247 - 2\log D - 0.4H$) of 0.07 and 0.08 that are among the lowest for any near-Earth asteroid. The radar observations occurred at the phase 0.40 in Fig. 1C near a minimum of the asteroid's lightcurve. This suggests that asteroid's long axis may have been oriented within a few tens of degrees of Earth during the radar observations, implying that the effective diameter may be larger than 0.64 km and that the radar and visual albedos may be even lower.

The upper bound on the radar albedo is consistent with those observed among BFGP- and C-type asteroids (Magri *et al.* 1999). Among near-Earth asteroids for which shape reconstructions have been published (4769 Castalia (Hudson and Ostro 1994), 6489 Golevka (Hudson *et al.* 2000), 4179 Toutatis (Hudson and Ostro 1995), 2063 Bacchus (Benner *et al.* 1999a), and 1620 Geographos (Hudson and Ostro 1999)), the upper bound on the radar albedo of 1999 GU_3 is comparable only to that of 1998 KY_{26} (Ostro *et al.* 1999b). The upper bound on the visual geometric albedo suggests the same taxonomic classes as the upper bound on the radar albedo (see Tholen and Barucci 1989). Although systematic errors due to uncertainties in extrapolation of high-phase-angle observations to zero phase could allow visual albedos greater than 0.10 that are marginally consistent with Q type suggested by the color indices, we conclude that no taxonomic class is consistent with all of the constraints. It is also possible, although unlikely, that the period is one-half of the estimate of 9 days. If so, then $D_{\max} \geq 0.32$ km and the upper bounds on the radar and visual geometric albedos (assuming $D_{\rm eff} = D_{\max}$) are 0.28 and 0.32, values that are consistent with the color indices.

4. Discussion. We interpret the 4.5-day period as one-half of the true rotation period because large-amplitude asteroid lightcurves are dominated by second harmonics. The rule that amplitudes of the first harmonic are smaller than amplitudes of the second harmonic has apparently been broken by only one large-amplitude lightcurve: the complex lightcurve of 4179 Toutatis in 1992–1993 showed just one deep minimum during the best-fit 7.3-day period obtained by Spencer *et al.* (1995). There were, however, observed multiple secondary minima between the primary minima in the lightcurve (see also Hudson and Ostro (1998) and Kryszczyńska *et al.* (1999)). Thus, the Toutatis lightcurve contained more than one minimum per period, as do all other known large-amplitude asteroid lightcurves. A 4.5-day rotation period of 1999 GU_3 showing only one minimum per rotation would be unique and there is no plausible theory how it could be generated. (A large hemispheric albedo difference is not plausible for the tiny world.) Thus, although we formally cannot exclude that the rotation period might be 4.5 days, we consider 9.0 days as the only plausible rotation period.

The 9-day rotation period exceeds more than 99% of all reported asteroid rotation periods (Pravec and Harris 2000). How did the slow rotation state of 1999 GU_3 originate? Among possible explanations are that the slow rotation resulted from the disruption of a larger progenitor, of which 1999 GU_3 is a fragment; from tidal interactions during one or more very close terrestrial planetary flybys (Richardson *et al.* 1998, Scheeres *et al.* 2000); from secular drag due to Yarkovsky thermal forces (Rubincam 2000); or due to a combination of these mechanisms. Another possibility is that the slow rotation is the result of tidal despinning between components of a direct binary system (Weidenschilling *et al.* 1989), possibly followed by removal of the secondary during a close encounter with a terrestrial planet, a scenario that could leave both components with rotation periods of up to several days (Farinella and Chauvineau 1993, Chauvineau *et al.* 1995). Recent studies suggested that binary asteroids are common among near-Earth asteroids (Pravec *et al.* 2000); thus there may be a source for slow rotators created by this mechanism. However, we find no evidence for a satellite in the radar data nor is there evidence for eclipses/occultations in the photometry.

Is 1999 GU_3 an NPA rotator? Impact simulations by Asphaug and Scheeres (1999) suggest that excitation of NPA rotation may be common among fragments of catastrophic disruptions; if so, then if 1999 GU_3 originated in a catastrophic disruption event, the question is whether enough time has elapsed for damping into a principal axis rotation state. A simple expression for estimating the damping timescale is $\tau \approx (P/C)^3/D_{\rm eff}^2$ (Harris 1994), where P is the sidereal rotation period in hours, $D_{\rm eff}$ is the effective diameter in kilometers, and C is a parameter that depends on the material properties of the asteroid. Using $D_{\rm eff} = 0.64$ km, $P = 216$ h, and $C = 17^{+23}_{-10}$, we obtain $\tau \approx 5^{+69}_{-4.6} \times 10^{12}$ yr, a timescale so long that it suggests that unless 1999 GU_3 originated in uniform rotation, it may be a NPA rotator. Thus, slow rotation and the deviation of two lightcurve points from simple periodicity might provide a hint of NPA rotation.

1999 GU_3 is currently near a temporary mean-motion resonance that brings the asteroid close to Earth every three years. The next opportunity for optical and radar observations of 1999 GU_3 occurs in April 2002, when the asteroid will approach within 0.081 AU of Earth and reach $V \approx 17$. Predicted SNRs at Arecibo are on the order of several thousand per day and should be strong enough to reconstruct the asteroid's detailed three-dimensional shape and to define the spin state.

Acknowledgments. This work was supported by the Grant Agency of the Academy of Sciences of the Czech Republic, Grant A3003708, and by the Grant Agency of the Czech Republic, Grant 205-99-0255. Part of this research was conducted at the Jet Propulsion Laboratory, California Institute of Technology, under contract with the National Aeronautics and Space Administration.

REFERENCES

Asphaug, E., and D. J. Scheeres 1999. Deconstructing Castalia: Evaluating a postimpact state. *Icarus* **139**, 383–386.

Benner, L. A. M., R. S. Hudson, S. J. Ostro, K. D. Rosema, J. D. Giorgini, D. K. Yeomans, R. F. Jurgens, D. L. Mitchell, R. Winkler, R. Rose, M. A. Slade, M. L. Thomas, and P. Pravec 1999a. Radar observations of asteroid 2063 Bacchus. *Icarus* **139**, 309–327.

Benner, L. A. M., S. J. Ostro, K. D. Rosema, J. D. Giorgini, D. Choate, R. F. Jurgens, R. Rose, M. A. Slade, M. L. Thomas, R. Winkler, and D. K. Yeomans 1999b. Radar observations of Asteroid 7822 (1991 CS). *Icarus* **137**, 247–259.

Binzel, R. P., P. Farinella, V. Zappalà, and A. Cellino 1989. Asteroid rotation rates: Distributions and statistics. In *Asteroids II* (R. P. Binzel, T. Gehrels, and M. S. Matthews, Eds.), pp. 416–441. Univ. of Arizona Press, Tucson.

Bowell, E., B. Hapke, D. Domingue, K. Muinonen, J. Peltoniemi, and A. W. Harris 1989. Application of photometric models to asteroids. In *Asteroids II* (R. P. Binzel, T. Gehrels, and M. S. Matthews, Eds.), pp. 524–556. Univ. of Arizona Press, Tucson.

Chamberlin, A. B., D. K. Yeomans, P. W. Chodas, J. D. Giorgini, R. A. Jacobson, M. S. Keesey, J. H. Lieske, S. J. Ostro, E. M. Standish, and R. N. Wimberly 1997. JPL solar system dynamics WWW site. *Bull. Am. Astron. Soc.* **29**, 1014. [Abstract]

Chauvineau, B., P. Farinella, and A. W. Harris 1995. The evolution of Earth-approaching binary asteroids: A Monte Carlo dynamical model. *Icarus* **115**, 36–46.

Dermott, S. F., A. W. Harris, and C. D. Murray 1984. Asteroid rotation rates. *Icarus* **57**, 14–34.

Farinella, P., and B. Chauvineau 1993. On the evolution of binary Earth-approaching asteroids. *Astron. Astrophys.* **279**, 251–259.

Farinella, P., D. R. Davis, P. Paolicchi, A. Cellino, and V. Zappalà 1992. Asteroid collisional evolution: An integrated model for the evolution of asteroid rotation states. *Astron. Astrophys.* **253**, 604–614.

Fulchignoni, M., M. A. Barucci, M. Di Martino, and E. Dotto 1995. On the evolution of the asteroid spin. *Astron. Astrophys.* **299**, 929–932.

Harris, A. W. 1979. Asteroid rotation rates II. A theory for the collisional evolution of rotation rates. *Icarus* **40**, 145–153.

Harris, A. W. 1994. Tumbling asteroids. *Icarus* **107**, 209–211.

Harris, A. W., J. W. Young, E. Bowell, L. J. Martin, R. L. Millis, M. Poutanen, F. Scaltriti, V. Zappalà, H. J. Schober, H. Debehogne, and K. W. Zeigler 1989. Photoelectric observations of Asteroids 3, 24, 60, 261, and 863. *Icarus* **77**, 171–186.

Harris, A. W., J. W. Young, E. L. G. Bowell, and D. J. Tholen 1999. Asteroid lightcurve observations from 1981–1983. *Icarus* **142**, 173–201.

Hudson, R. S., and S. J. Ostro 1994. Shape of Asteroid 4769 Castalia (1989 PB) from inversion of radar images. *Science* **263**, 940–943.

Hudson, R. S., and S. J. Ostro 1995. Shape and non-principal axis spin state of asteroid 4179 Toutatis. *Science* **270**, 84–86.

Hudson, R. S., and S. J. Ostro 1998. Photometric properties of Asteroid 4179 Toutatis from lightcurves and a radar-derived physical model. *Icarus* **135**, 451–457.

Hudson, R. S., and S. J. Ostro 1999. Physical model of Asteroid 1620 Geographos from radar and optical data. *Icarus* **140**, 369–378.

Hudson, R. S., and 26 colleagues 2000. Radar observations and physical model of asteroid 6489 Golevka. *Icarus*, in press.

Kryszczyńska, A., T. Kwiatkowski, S. Breiter, and T. Michalowski 1999. Relation between rotation and lightcurve of 4179 Toutatis. *Astron. Astrophys.* **345**, 643–645.

Landolt, A. U. 1992. UBVRI photometric standard stars in the magnitude range $11.5 < V < 16.0$ around the celestial equator. *Astron. J.* **104**, 340–371.

Magri, C., S. J. Ostro, K. D. Rosema, M. L. Thomas, D. L. Mitchell, D. B. Campbell, J. F. Chandler, I. I. Shapiro, J. D. Giorgini, and D. K. Yeomans 1999. Mainbelt asteroids: Results of Arecibo and Goldstone radar observations of 37 objects during 1980–1995. *Icarus* **140**, 379–407.

Mottola, S., W. D. Sears, A. Erikson, A. W. Harris, J. W. Young, G. Hahn, M. Dahlgren, B. E. A. Mueller, B. Owen, R. Gil-Hutton, J. Licandro, M. A. Barucci, C. Angeli, G. Neukum, C.-I. Lagerkvist, and J. F. Lahulla 1995. The slow rotation of 253 Mathilde. *Planet. Space Sci.* **43**, 1609–1613.

Ostro, S. J., D. B. Campbell, R. A. Simpson, R. S. Hudson, J. F. Chandler, K. D. Rosema, I. I. Shapiro, E. M. Standish, R. Winkler, D. K. Yeomans, R. Velez, and R. M. Goldstein 1992. Europa, Ganymede, and Callisto: New radar results from Arecibo and Goldstone. *J. Geophys. Res.* **97**, 18,227–18,244.

Ostro, S. J., R. S. Hudson, K. D. Rosema, J. D. Giorgini, R. F. Jurgens, D. K. Yeomans, P. W. Chodas, R. Winkler, R. Rose, D. Choate, R. A. Cormier, D. Kelley, R. Littlefair, L. A. M. Benner, M. L. Thomas, and M. A. Slade 1999a. Asteroid 4179 Toutatis: 1996 radar observations. *Icarus* **137**, 122–139.

Ostro, S. J., P. Pravec, L. A. M. Benner, R. S. Hudson, L. Šarounová, M. D. Hicks, D. L. Rabinowitz, J. V. Scotti, D. J. Tholen, M. Wolf, R. F. Jurgens, M. L. Thomas, J. D. Giorgini, P. W. Chodas, D. K. Yeomans, R. Rose, R. Frye, K. D. Rosema, R. Winkler, and M. A. Slade 1999b. Radar and optical observations of Asteroid 1998 KY_{26}. *Science*, **285**, 557–559.

Pravec, P., and A. W. Harris 2000. Fast and slow rotation of asteroids. *Icarus*, in press.

Pravec, P., L. Šarounová, D. L. Rabinowitz, M. D. Hicks, M. Wolf, Yu. N. Krugly, F. P. Velichko, V. G. Shevchenko, V. G. Chiorny, N. M. Gaftonyuk, and G. Genevier 2000. Two-period lightcurves of 1996 FG_3, 1998 PG and (5407) 1992 AX: One probable and two possible binary asteroids. *Icarus* **146**, 190–203.

Pravec, P., L. Šarounová, and M. Wolf 1996. Lightcurves of 7 near-Earth asteroids. *Icarus* **124**, 471–482.

Pravec, P., M. Wolf, and L. Šarounová 1998. Lightcurves of 26 near-Earth asteroids. *Icarus* **136**, 124–153.

Rabinowitz, D. L. 1998. Size and orbit dependent trends in the reflectance colors of Earth-approaching asteroids. *Icarus* **134**, 342–346.

Richardson, D. C., W. F. Bottke, and S. G. Love 1998. Tidal distortion and disruption of Earth-crossing asteroids. *Icarus* **134**, 47–76.

Rubincam, D. P. 2000. Radiative spin-up and spin-down of asteroids. *Icarus* **148**, 2–11.

Scheeres, D. J., S. J. Ostro, R. A. Werner, E. Asphaug, and R. S. Hudson 2000. Effects of gravitational interactions on asteroid spin states. *Icarus* **147**, 106–118.

Spencer, J. R., L. A. Akimov, C. Angeli, P. Angelini, M. A. Barucci, P. Birch, C. Blanco, M. Buie, A. Caruso, V. G. Chiornij, F. Colas, P. Dentchev, M. C. De Sanctis, E. Dotto, M. Fulchignoni, S. Green, A. Harris, T. Hudeček, A. V. Kalashnikov, V. V. Kobelev, V. P. Kozhevnikov, Y. Krugly, D. Lazzaro, J. Lecacheux, J. MacConnell, T. Michalowski, R. A. Mohamed, B. Mueller, T. Nakamura, C. Neese, K. Noll, W. Osborn, P. Pravec, D. Riccioli, V. Shevchenko, D. Tholen, F. Velichko, C. Venditti, R. Venditti, W. Wisniewski, J. Young, and B. Zellner 1995. The lightcurve of 4179 Toutatis: Evidence for complex rotation. *Icarus* **117**, 71–89.

Tholen, D. J., and M. A. Barucci 1989. Asteroid taxonomy. In *Asteroids II* (R. P. Binzel, T. Gehrels, and M. S. Matthews, Eds.), pp. 1139–1150. Univ. of Arizona Press, Tucson.

Veverka, J., P. Thomas, A. Harch, B. Clark, J. F. Bell III, B. Carcich, J. Joseph, C. Chapman, W. Merline, M. Robinson, M. Malin, L. A. McFadden, S. Murchie, S. E. Hawkins III, R. Farquhar, N. Izenberg, and A. Cheng 1997. NEAR's flyby of 253 Matilde: Images of a C asteroid. *Science* **278**, 2109–2114.

Weidenschilling, S. J., P. Paolicchi, and V. Zappalà 1989. Do asteroids have satellites? In *Asteroids II* (R. P. Binzel, T. Gehrels, and M. S. Matthews, Eds.), pp. 643–658. Univ. of Arizona Press, Tucson.